

Charpy Impact Response of the Cracked Aluminum Plates Repaired with FML Patches using the Response Surface Methodology

Faramarz Ashenai Ghasemi^{#,*}, Lotfali Mozaffari Vanani[#], Ali Pourkamali Anaraki[#], and Sadigh Raissi[§]

[#]Department of Mechanical Engineering, Shahid Rajaei Teacher Training University, Tehran, Iran

[§]Department of Industrial Engineering, Islamic Azad University, Tehran, Iran

*E-mail: f.a.ghasemi@srutu.edu

ABSTRACT

Here, the effect of fiber metal laminate (FMLs) patches was studied for repairing of single-sided cracked aluminum plates experimentally to see their response to Charpy impact tests. The main desired parameters were composite patch lay-up, crack length, and crack angle each one in three levels. All experimental attempts generated and followed based on the design of experiments method by using of response surface methodology. The predicted energy absorption values obtained from the model were in good agreement with the experimental results. No matter the specimens were repaired or not, as the crack length was increased the energy absorption of the structure was decreased. The experimental results also showed that for lengthen cracks, increasing of the crack angle had more effect on energy absorption. Also it was observed that the patch lay-up effective on the impact response of the specimens. The more the metal layer was departed from the aluminum plate and the FML patches interfacial surface, the less energy was absorbed in the structure.

Keywords: Cracked aluminum plate, Charpy impact test, FML patch, response surface methodology

1. INTRODUCTION

Different methods have been used to improve the lifetime of the cracked structures. One of these methods is using of adhesively bonded composite patches to repair a cracked component. This was initially examined by the Aeronautical and Maritime Research Laboratories (AMRL) for the Royal Australian Air Force (RAFF)¹ in 1970s.

Schubbe², *et al.* conducted an investigation to show the post-repair fatigue crack growth behaviour in aluminum plates repaired with the asymmetrically bonded full width boron/epoxy composite patch. They found that for a special patch length, an increase in the stiffness ratio improves the fatigue life of the thick or thin repaired plates. They also showed that asymmetric repair results inconsiderable curvature or elementary bending after attaching of patch in thick repaired plates, and these effects depended on the patch configurations. They also found that debond growth was dependent on the crack length rather than on the patch configuration. Wang³ described the modeling of a repaired structure by shape memory alloy (SMA) wire embedded composite patches, and evaluated the closure stress. They understand that an increase in patch thickness and a reduction in the matrix modulus improves the closure stress. They also demonstrated that the maximum closure stress generated by these patches is highly influenced by the ratio of the patches to the repaired structures thickness, and it is also significantly dependent to the bonding strength of the

composite matrix and SMA wires. Belhouari⁴, *et al.* performed the finite element method to see the advantage of using of the bonded symmetric composite patch for repairing cracks in metallic sheets in mode I and mixed mode. Their results showed that by using of a double symmetric patch respect to a single patch, there will be a considerable reduction of the asymptotic magnitude of the stress intensity factor at the tip of crack. They showed that the use of the double patch reduces appreciably the stress intensity factor compared to single patch. They demonstrated that an increase in thickness develops with the crack length and it reduces when the thickness of the patch enlarges. For small length this increase can exceed largely 50 per cent at the asymptotic value of the stress intensity factor (SIF).

Tsai⁵, *et al.* performed stresses analyses for various aluminum plates, having no crack, a crack, a crack and a single-side composite patch, as well as a crack and a double-side composite patch. They performed SIF and fatigue life calculations for these situations: a cracked plate and a repaired one. They showed that the stress in the aluminum plate with and without a crack was very different, with the stress in the aluminum plate with a crack being much higher than that of the aluminum plate without crack. They found that the stress along the thickness was not the same; and the stress variation did not maintain the same route for different crack lengths. They showed that for single-side repaired aluminum plate, the stresses through the thickness are significantly different and the biggest stress intensity factor was obtained at the composite patching side. Ghosh⁶, *et al.* presented a

new finite element (FE) formulation for laminates having magnetostrictive patches using an hysteretic, coupled, linear properties of magnetostrictive materials. They showed that the layer sequence has an important effect on the samples behaviour.

Toudeshky⁷, *et al.* studied the fatigue crack growth of composite patches reinforced panels having mixed-mode cracks. They obtained the crack trajectories using dynamic mesh generation for repaired panels. They showed that the fatigue crack growth life of the repaired plates in mode-I is nearly correspondent with the experiments. They also find that the thickness of patch has not important on path of the crack propagation. There are significant differences between the obtained life using un-patched surface and mid-plane fracture parameters for different thicknesses of patches and ply angles of the repaired plates. Papanikos⁸, *et al.* used a FE-based progressive failure model to study the patch debonding initiation and improvement resulted from mechanical loading. They applied a metallic plate having a central crack loaded in tension and repaired using a double-sided rectangular tapered composite patch. They found that, depending to the patch thickness, the debonding begins at the upper patch edge or at the crack faces. They investigated that, the initiation load of debonding increases by increasing of the thickness of patches, adhesive thickness and tapered length. Ayatollahi⁹, *et al.* used a three-dimensional FEM of the single-sided repaired plate to see the effect of patching. They used the generalised maximum tangential stress criterion to predict the fracture initiation angle and the fracture strength of repaired crack. They showed that bonding a composite patch reduces the stress intensity factors. They claimed that the mode I reduction factor decreases when the crack line tends to the loading directions. They demonstrated that the fracture initiation angle of a crack is affected a little because of a composite patch.

Khalili¹⁰, *et al.* experimentally studied the repaired aluminum plates with composite patches by Charpy impact test. They showed that carbon patches are reinforces the cracked plates more than the glass ones. They also investigated that when the crack length to specimen width ratio is constant, the carbon patches behave better than glass ones. Khalili¹¹, *et al.* studied repaired aluminum specimens by metallic, composite, and FML patches using of Charpy impact tests. They found that FML patches are more effective in reinforcing the notched specimens than GFRP (glass-fiber reinforced plastic) and CFRP patches. They showed that an increase in the notch length, decreases the absorbed energy of the un-repaired specimens. They also demonstrated that in the specimens with composite patches, no matter what the number of layers are, the fiber type has an important role in energy absorption, although with the FML patches, the number of layers is important.

Pandey and Kumar¹² showed that composite patch repairs of cracked metallic aircraft structures extend their life. They presented the numerical calculation into the interface behavior of repaired aluminum alloy plates patched by fiber composites. They modelled adhesive as an elasto-plastic bilinear material to characterise the debond behaviour. They selected two patch shapes. They performed material and geometric nonlinear analyses for different type of patches to find the peel and shear

stresses between the substrate and the patch to find the feasibility of delamination/debonding interface. They also parametrically studied the effect of adhesive and patch thickness to predict their effect on damage toleration of repaired structures.

Here, experiments were done to see the effect of the single-sided repaired aluminum plates using the FML patches. Charpy impact tests were used to see the effect of repairing the structures. The composite patches were made of metal and polymer composite layers. Three different crack lengths, angles and patch lay-ups were studied. To find the different between the energy absorption mechanism of repaired and un-repaired cracked specimens, some experiments were done.

2. RESPONSE SURFACE METHODOLOGY

A mathematical model related to the response value to the levels of three factors is a vital aid in the explanation of results from a set of design experiments. Generally many investigators tend to fit a simple regression model to the experiments such as follow as¹³:

$$y = \beta_0 + \beta_1x_1 + \beta_2x_2 + \beta_3x_3 + e \tag{1}$$

where y nominates each response and x_1, x_2, x_3 show factors, β_j called as regression coefficients and e model's error term. Wide experience has shown that quadratic relationships are usually adequate. Based on this, the following general form of a second degree polynomial relating to each of responses was assumed such as:

$$y = \beta_0 + \beta_1\beta x_1 + \beta_2x_2 + \beta_3x_3 + \beta_{12}\beta x_1x_2 + \beta_{13}x_1x_3 + \beta_{23}x_2x_3 + \beta_{11}x_1^2 + \beta_{22}x_2^2 + \beta_{33}x_3^2 + e \tag{2}$$

The following quadratic function may be written in linear form by assist of a few transformations to convert it as:

$$y = \beta_0 + \beta_1\beta x_1 + \beta_2x_2 + \beta_3x_3 + \beta_4x_4 + \beta_5x_5 + \beta_6x_6 + \beta_7x_7 + \beta_8x_8 + \beta_9x_9 + e \tag{3}$$

where $x_4 = x_1x_2, x_5 = x_1x_3, x_6 = x_2x_3, x_7 = x_1^2, x_8 = x_2^2,$ and $x_9 = x_3^2$. In this case, the full three variable quadratic functions will be expressed by a linear nine variable function or in general by a linear k -variable regression form which may express by a matrix notation as follow as:

$$y = X\beta + \epsilon \tag{4}$$

or in expanded form:

$$\begin{bmatrix} y_1 \\ y_2 \\ 0 \\ 0 \\ 0 \\ y_n \end{bmatrix} = \begin{bmatrix} 1 & x_{11} & x_{12} & 0 & 0 & x_{1k} \\ 1 & x_{21} & x_{22} & 0 & 0 & x_{2k} \\ 0 & 0 & 0 & 0 & 0 & 0 \\ 0 & 0 & 0 & 0 & 0 & 0 \\ 0 & 0 & 0 & 0 & 0 & 0 \\ 1 & x_{n1} & x_{n2} & 0 & 0 & x_{nk} \end{bmatrix} \begin{bmatrix} B_0 \\ B_1 \\ 0 \\ 0 \\ 0 \\ B_k \end{bmatrix} + \begin{bmatrix} \epsilon_1 \\ \epsilon_2 \\ 0 \\ 0 \\ 0 \\ \epsilon_n \end{bmatrix} \tag{5}$$

The least square estimator of the coefficients is:

$$\hat{\beta} = (X'X)^{-1}X'y \tag{6}$$

Using a standard computer program all the coefficients, the relevant tables, graphs and adequacy indices may be computed for the responses. It is always necessary to examine the fitted model to ensure that it provides an adequate approximation to the true system and verifying that none of the least squares regression assumptions are violated.

3. SPECIMENS AND FML PATCHES PREPARATION

3.1 Cracked Aluminum Plates

In this study, aluminum alloy plate¹⁴ AA1035 having the thickness of 3 mm was used for the cracked specimens. The mechanical properties of this sheet are determined by tensile test ASTM¹⁵ E8m-09-2010 and they are shown in Table 1. In order to prepare the specimens from the metal sheet in principle dimensions, 70 mm × 15.3 mm, the water jet machine was used. To produce the crack on single edge of the specimens, wire cut machine was used. The width of wire cutting was 0.25 mm.

Two main parameters of crack characteristics that influenced on the Charpy impact resistance of the specimens were crack length and crack angle. Therefore, three different crack lengths and angles were considered. The crack lengths were chosen so that the crack lengths to the specimen width (a/w ratio or crack length ratio) had the amounts of $a/w = 0.1, 0.3,$ and 0.5 . Therefore, the crack lengths were equal to 1.52 mm, 4.56 mm and 7.6 mm (Fig. 1). The crack angles with respect to the width axis of specimens were equal to $0^\circ, 30^\circ$ and 45° (Fig. 2). The specimens with same crack configuration in length and angle were kept together and then wire cut. The different specimen configurations from the crack length ratios and crack angles point of view are depicted in Fig. 2.

3.2 FML Patches

The number of patch layers supposed to be fixed as three layers. Two layers of woven glass-fabric (T(90)/M200-E10) material as the glass-fiber reinforced composite layers and one thin aluminum sheet (AA1035) having 0.3 mm thickness, as the metal layer. Except the crack length and the crack angle, the third parameter that was studied in this research was the patch lay-up. The FML patches were made so that they had three different lay-ups, and every one of these lay-ups was named by a code. The specimens had FML patch lay-up of G-G-A (G shows the glass fiber reinforced plastic and A shows the aluminum layer), from bottom to up direction (the C1 repair code was assigned for this case). It means that in C1 repair type, the glass fiber reinforced plastic layers are bonded to the cracked plate and the aluminum layer is at the farthest place from the repair surface. In second repaired specimens with code C2, the patch lay-up was A-G-G, and finally in patches with code C3 the lay-up was G-A-G. As it is seen, in C2 type

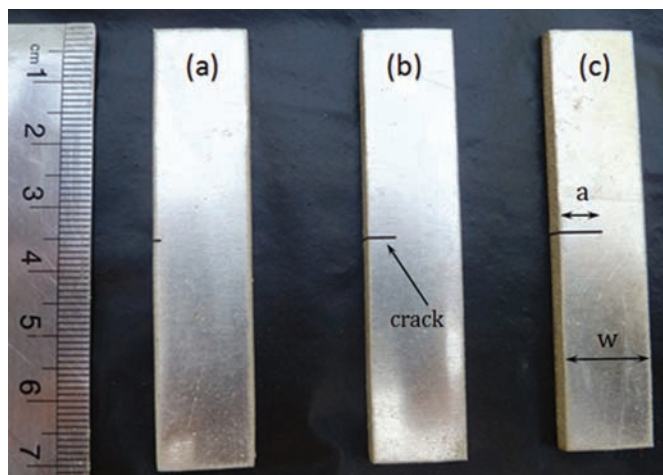


Figure 1. Specimens with different crack length ratios: (a) $a/w=0.1$, (b) $a/w=0.3$ and (c) $a/w=0.5$.

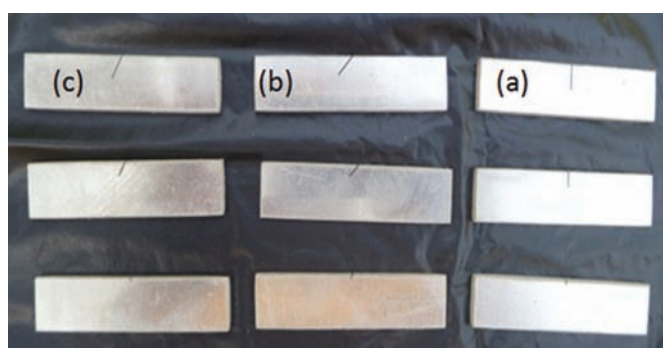


Figure 2. Specimens with different crack angles (a) $\theta=0^\circ$, (b) $\theta=45^\circ$, and (c) $\theta=30^\circ$.

patches the aluminum layer is fully attached to the metal plate, and in C3 type patches the aluminum layer is in the middle of patch lay-up. The fibers angle in the patches lay-ups are equally along 0° and 90° in all of them. To bond the glass fiber reinforced plastic and the aluminum layers strongly, the surfaces must be prepared. Bonding of the aluminum layer surfaces was done according to ASTM E 23 – 02a¹⁶. The epoxy (LY5052-Huntsman Corporation) was used as matrix in the GFRP layers due to its good performance for aerospace industries¹⁷. The average fiber content was about 55 per cent by weight in glass fiber reinforced plastic layers. The composite patches were made by hand and then the curing procedure according to the recommended cure schedule in two stages was done¹⁷. At first the patches were cured in 60°C for 2 h and then in 80°C for 4 h in the oven rig. The patches dimensions were $40\text{ mm} \times 10\text{ mm}$ and after curing their thickness became 0.8 mm. Araldite 2015 was employed to bond the patches to the cracked plates¹⁷. The adhesive layer had a thickness about 0.2 mm. Surface preparation procedure of aluminum layer of patch was done according to the P2 etching process (as mentioned before), before bonding the patches to the cracked plates. For bonding glass fiber reinforced plastic layer, the surface preparation was done according to the procedure recommended for thermoset materials¹⁸. Table 1 shows the mechanical

Table 1. Material properties of the aluminum plate, the patches, and the adhesive

	Elastic modulus	Shear modulus	Ultimate tensile strength	Density	Poisson's ratio
	$E_x=E_y$ (GPa)	G_{xy} (GPa or MPa)	$S_x=S_y$ (MPa)	P (g/cm ³)	ν_{xy}
Aluminum-AA1035	69	26(GPa)	157	2.7	0.3
Epoxy-LY5052	3.5	-----	60	1.16	0.35
GFRP layer	16	-----	230	1.6	0.25
Araldite-2015	2	10-20(MPa)	30	1.4	-----

properties of the aluminum plate, patches, and bonding material.

To have proper specifications of specimens for patching them and quick referencing of the specimens for results recording and subsequent discussions, an experiments table was created (Table 2). In this table different specimen configurations from the repair patch type, crack length ratios and crack angles point of view are shown.

From Table 2 it is seen that every specimen has a unique code. In this coding letters U and C show the un-cracked and cracked specimens, respectively. After the letter C, there are three digits. The first digit indicates that if the specimens are repaired with a patch (digits 1, 2, or 3) or not (digit 0). The second digit shows the crack length ratios. For a/w ratio=0.1, 0.3, and 0.5 we take digits 1, 2, and 3 respectively. Finally the third digit indicates the crack angle. For angles 0°, 30°, and 45° we take digits 1, 2, and 3 respectively. For example, the specimen having C231 code indicates a specimen reinforced with FML patch by A-G-G lay-up (C2 patch type), a crack length of 7.65 mm (a/w ratio=0.5) and a crack angle of 0°. As an another example, C031 is a specimen with the same crack characteristics as C131, C231, and C331 from crack length ratio and angle points of view; except that C031 is not repaired with any type of patches. These are described briefly in Table 3.

The patches were made separately and then bonded to the specimens according to the design of experiments table (Table 4). Figure 3 shows the specimens that are un-cracked (a), cracked but un-repaired (b), and finally cracked and repaired (c).

3.3 Adhesive

The adhesive Araldite2015 was selected for bonding the FML patches to the cracked plates. This is due to its good property of bonding¹⁹. The thickness of the adhesive layer was kept about 0.2 mm. In order to have a complete bonding between the specimens and FML patches, the specimens’ surface should be prepared before patch bonding. This preparation had a procedure according to the P2etching process²⁰. In this manner the bonding surface of the aluminum plate is firstly degreased with acetone, and then abraded with emery cloth. Finally, alkaline cleaning was applied. Thereafter the specimens were immersed for 12 min at 65-70 °C P2 etch mixture of 15 per cent by weight FeSO₄, 37 per cent H₂SO₄ and 48 per cent water. They were washed with the clean cold running water, followed by clean hot water and then they were dried with hot air. The temperature of the hot water and air must be less than²¹ 65 °C. Also for the patches having C2 code, the same surface preparation procedure as P2 etching process was conducted because the metal layer should be bonded to the cracked plate.

4. CHARPY IMPACT TESTS

An impact test can be used to assess the material’s fracture resistance. In this test, a pendulum is mounted is dropped from a known height (h_1) to impact a sample

at the bottom of its arc. Therefore, the material is subjected to a high strain rate. Therefore, it experiences the fracture rather than the flow. This is a standard high strain rate test that determines the value of the absorbed energy by a material during fracture. .

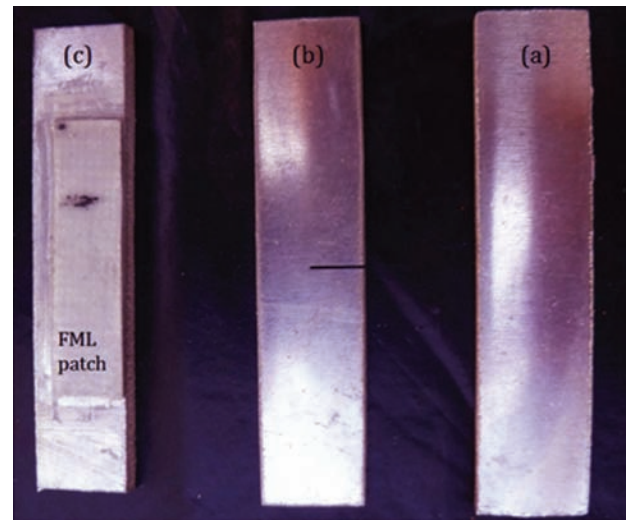


Figure 3. Specimens (a) un-cracked, (b) cracked but un-repaired and (c) cracked and repaired with a FML patch.

Table 2. Experiments table according to DOE method

Test no.	Specimens codes	Patch lay-ups	Crack length ratios (a/w ratios)	Crack angles (°)
1	U	Un-repaired	Un-cracked	Un-cracked
2	C011	Un-repaired	0.1	0
3	C211	A-G-G		
4	C012	Un-repaired		
5	C112	G-G-A	0.1	30
6	C312	G-A-G		
7	C013	Un-repaired	0.1	45
8	C213	A-G-G		
9	C021	Un-repaired		
10	C121	G-G-A	0.3	0
11	C321	G-A-G		
12	C022	Un-repaired	0.3	30
13	C222	A-G-G		
14	C023	Un-repaired		
15	C123	G-G-A	0.3	45
16	C323	G-A-G		
17	C031	Un-repaired	0.5	0
18	C231	A-G-G		
19	C032	Un-repaired		
20	C132	G-G-A	0.5	30
21	C332	G-A-G		
22	C033	Un-repaired	0.5	45
23	C233	A-G-G		

Table 3. The meaning of the C digits

The location of the C digits	Related parameter	Digit	Concept
First digit	Patch lay-up (Repair type)	0	Un-repaired
		1	G-G-A
		2	A-G-G
		3	G-A-G
Second digit	Crack length ratios (a/w ratios)	1	$a/w=0.1$
		2	$a/w=0.3$
		3	$a/w=0.5$
Third digit	Crack angle ($^\circ$)	1	0
		2	30
		3	45

Table 4. Definition of the desired parameters and their related levels used in RSM

Variable	Symbol	Coded variable levels		
		Low	Center	High
		-1	0	1
FML patch lay-up	X_1	G-G-A	A-G-G	G-A-G
Crack length ratios (a/w ratios)	X_2	0.1	0.3	0.5
Crack angle	X_3	0°	30°	45°

The Charpy tests were done according to ASTM E23-02a²². Figure 4(a) shows the Charpy impact test machine that was used for the experiments. The pendulum hammer had a mass of 15.200 kg and the radius of its disc was 150 mm. The mass and swing arm length were 5.270 kg and 520 mm, respectively. This leads to a stored energy of about 218.5 J and a speed at the impact point of about 5.033 m/s. The waste friction energy was about 1.9 J and waste energy of air resistance was neglected. The final absorbed energy of each specimen was the average of three samples. Figure 4(b) presents an impact test specimen for testing.

5. RESULTS AND DISCUSSIONS

5.1 The Experimental Analysis

At first, un-cracked specimen was tested and its energy

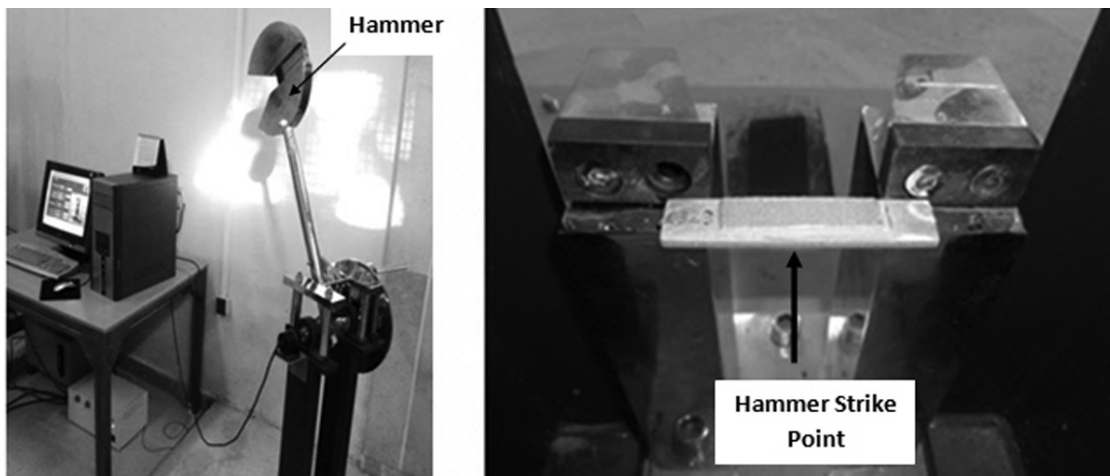


Figure 4. (a) Charpy test device and (b) the prepared specimen for testing.

absorption acquired to 53.00 J. Then nine types of un-repaired cracked specimens were tested. Different cracks have different effects on specimens' strength. The results of un-repaired cracked specimens are shown in Fig. 5. It is clear that by increasing the crack length ratio, the specimen strength and consequently the energy absorption will be decreased.

Figure 5 also shows that the more the crack angle is, the more energy absorbs in the structure. The most energy is absorbed in the specimens with a crack angle of 45° . This is because of crack growth path change that powers the crack to go in first mode of fracture. This change in direction leads to a more energy absorption too. By increasing the crack length ratio, the energy absorption grows by changing the crack angle from 0° to 45° . Figure 5 shows that if the crack angle changes from 0° to 45° , the energy absorption of un-repaired specimens with a crack length ratio of $a/w=0.5$ increases about 21 per cent. Similarly, this difference for $a/w=0.3$ and $a/w=0.1$ ratios are 9 per cent and 2 per cent, respectively. Because by extending the crack length ratio, the path that the crack should go to attain the first mode of fracture enlarges. So, the value of absorbed energy increases too.

Here, the main factors for the un-repaired cracked specimens are the plastic deformation and 45° shear surface as shown in Figs. 6 and 7, respectively. The fracture of the patched specimens was almost similar to the un-patched ones. The main phenomenon in the patches was fiber breakage, fiber pull out of glass fiber reinforced plastic layer and plastic deformation of the aluminum layer of the patches (Fig. 8).

5.2 Response Surface Analysis

According to Table 2, the patches were joined to the specimens with different crack angles and crack length ratios that were mentioned earlier. They were tested to see how the effects of patch lay-up and crack properties are in the strength of the repaired samples. The response of any regimes in the interval of our experiment design could be calculated from Eqn. (1). The predicted values of energy absorption were compared with the experimental results (Table 5). Table 5 shows a good estimation of the energy absorption values (obtained by the presented method) shows compared to the experimental results.

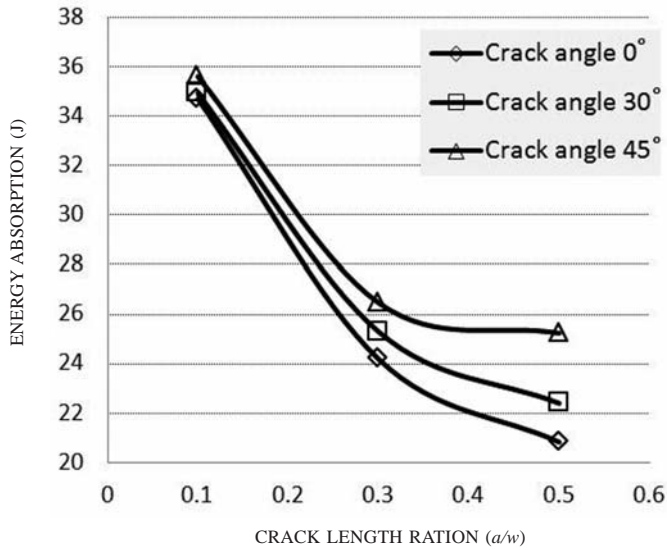


Figure 5. Energy absorption of the un-repaired cracked specimens.

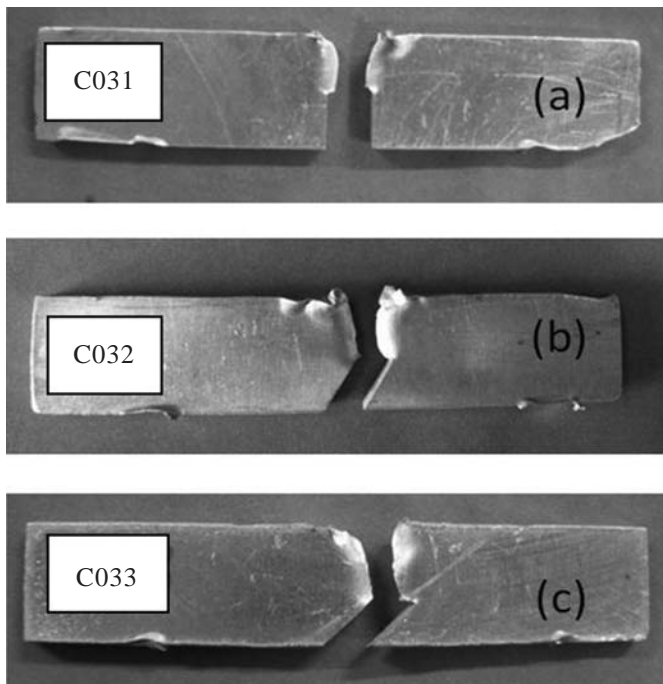


Figure 6. Crack trajectory in different crack angles for a constant crack length ratio of $a/w = 0.5$ and (a) $\theta = 0^\circ$, (b) $\theta = 30^\circ$, (c) $\theta = 45^\circ$.

By using SPSS statistical package, the final least square parameter estimations were identified as Table 6. Table 6 shows that X_1 , X_2 , X_3 and X_1^2 are significant and should be involved on the response surface equation as shown in Eqn 7:

$$Y = 32.166 + 0.969 X_1 - 5.764 X_2 + 2.741 X_3 - 1.819 X_1^2 \quad (7)$$

where Y is the predicted response and X_1 , X_2 and X_3 are different independent variables that represent the FML patch type, crack length ratio and crack angle, respectively. The response variables could vary between -1 to +1 that their coded were defined in Table 4.

The variance analysis of Eqn. (7) is presented in Table 7. To test the fit of the model, the regression equation and

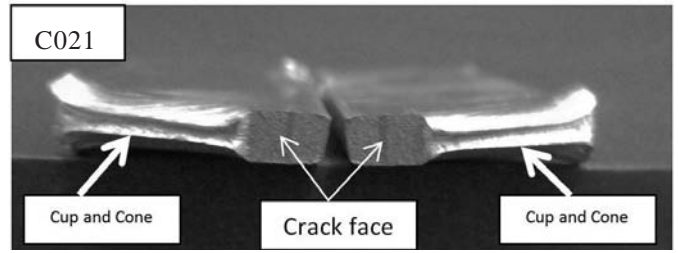


Figure 7. Shear surface of a broken C021 specimen.

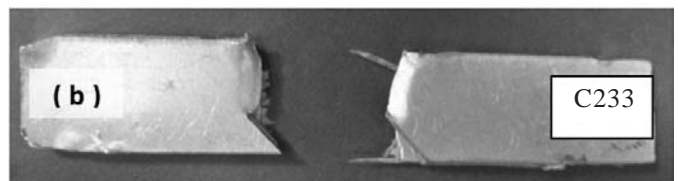
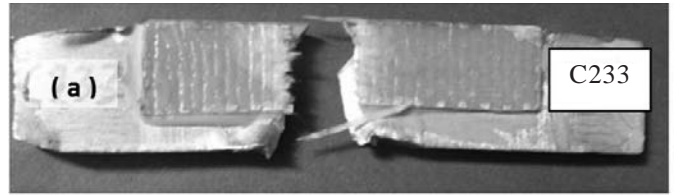


Figure 8. Different view of a repaired specimen after the fracture: (a) front view of C233 type, (b) back view of C233 type.

determination coefficient (R^2) were measured. The model F-value of 50.623 shows that the model is important. There is roughly zero percent chance that this large F-value occurs due to noise alone. The low probability value in last column of Table 7 shows that the model is considerable. The model was tested by the determination coefficient ($R^2 = 0.914$), which offers that more than 91.4 per cent of the variance is ascribable to the variables and also shows that the model is very important.

Figure 9 presents the studentised residuals and normal percent probability plot. Residuals show the differences between the considered amount of a response measurement and the value that is fitted by model. The model prediction is precise as the residual values are small.

In order to gain a better understanding of the results, the predicted model is represented in Figs. 10-12, as the 3D response surface plots. Figure 10 shows the effect of crack angle and crack length ratio on the specimen energy absorption for different FML patch types. There is an important correlation between the angle and length of crack with the value of specimens' absorbed energy. As the crack length ratio increases, the fracture energy of the structure reduces. But, when by crack angle increases, the strength of the specimens grows too. The most significant hint is the differences of absorbed energy values of different repairs. The reason is that by varying of the patch lay-up, the value of the absorbed energy of the structure varies too. By checking the results (especially the graphs), one sees that the aluminum layer place has an important role on the repair performance. If the place of the aluminum layer is near of the base structure (repair type C2), the more energy absorbs in it.

This happens as the fracture mechanism changes in the

Table 5. Codified levels for the experimental and predicted results for energy absorption

Tests no.	Actual and coded level of variables			Experimental results (J) Y	Predicted results (J) Y	Percent of error between experimental and predicted results
	X ₁ (FML patch lay-ups)	X ₂ (a/w)	X ₃ (Crack angles)			
1	1(G-A-G)	0(0.3)	1(45°)	34.56	34.05	1.5
2	1(G-A-G)	-1(0.1)	0(30°)	36.91	37.08	0.46
3	1(G-A-G)	0(0.3)	-1(0°)	27.63	28.57	3.29
4	0(A-G-G)	0(0.3)	0(30°)	31.69	32.16	1.46
5	0(A-G-G)	-1(0.1)	1(45°)	40.61	40.67	0.15
6	1(G-A-G)	1(0.5)	0(30°)	26.15	25.55	2.35
7	0(A-G-G)	1(0.5)	1(45°)	29.5	29.14	1.24
8	0(A-G-G)	-1(0.1)	-1(0°)	36.5	35.18	3.75
9	-1(G-G-A)	0(0.3)	1(45°)	31.46	32.11	2.02
10	-1(G-G-A)	1(0.5)	0(30°)	24.09	23.61	2.03
11	0(A-G-G)	1(0.5)	-1(0°)	23.48	23.66	0.76
12	-1(G-G-A)	0(0.3)	-1(0°)	26.61	26.63	0.08
13	-1(G-G-A)	-1(0.1)	0(30°)	35.34	35.14	0.57

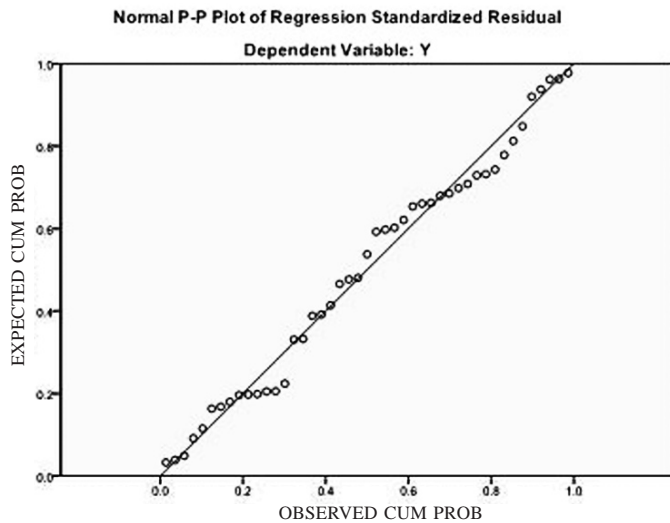


Figure 9. Normalised residuals plot of energy absorption.

various patches. When the aluminum layer is far from the repaired surface, the brittleness of the whole structure becomes more. Therefore, the structure absorbs the less energy. When the aluminum layer is placed in the middle of patch lay-up or even more near to the repaired surface, the ductile fracture improves. One sees that the value of the loading and the required time of aluminum layer plasticity are too low. So, the more the aluminum layer is near to the repaired surface, the more the structure shows a ductile behavior. It can be noted that if the structure is repaired with the C2 type patches, regardless of what the crack angle or crack length ratio is, the specimens reach their maximum strength.

The effects of FML patch type and crack angle on energy absorption for different crack length ratios were showed in Fig. 11. The degrees of the curves Fig. 11 is 2, respect to the X₁ axis. Also at point 0 that the patch type is C2 (A-G-G lay-up), the amount of the absorbed energy of the structure is the most, regardless of the crack length ratio. An increase in the crack

Table 6. The coefficients of the predicted equation (Eqn 7) based on the standard SPSS report

Model		Un-standardised Coefficients		Standardised Coefficients	t	Sig.	Co-linearity Statistics	
		B	Std. Error	Beta			Tolerance	VIF
1	(Constant)	32.166	.494		65.129	.000		
	X ₁	.969	.462	.135	2.098	.042	1.000	1.000
	X ₂	-5.764	.462	-.801	-12.476	.000	1.000	1.000
	X ₃	2.741	.462	.381	5.934	.000	1.000	1.000
	X ₁ squared	-1.819	.676	-.173	-2.689	.010	1.000	1.000

Table 7. Analysis of variance for response surface quadratic model

Model		Sum of Squares	df	Mean Square	F	Sig.
1	Regression	1037.235	4	259.309	50.623	0.000 ^a
	Residual	204.894	40	5.122		
	Total	1242.128	44			

a. Predictors: (Constant), X₁squared, X₃, X₂, X₁

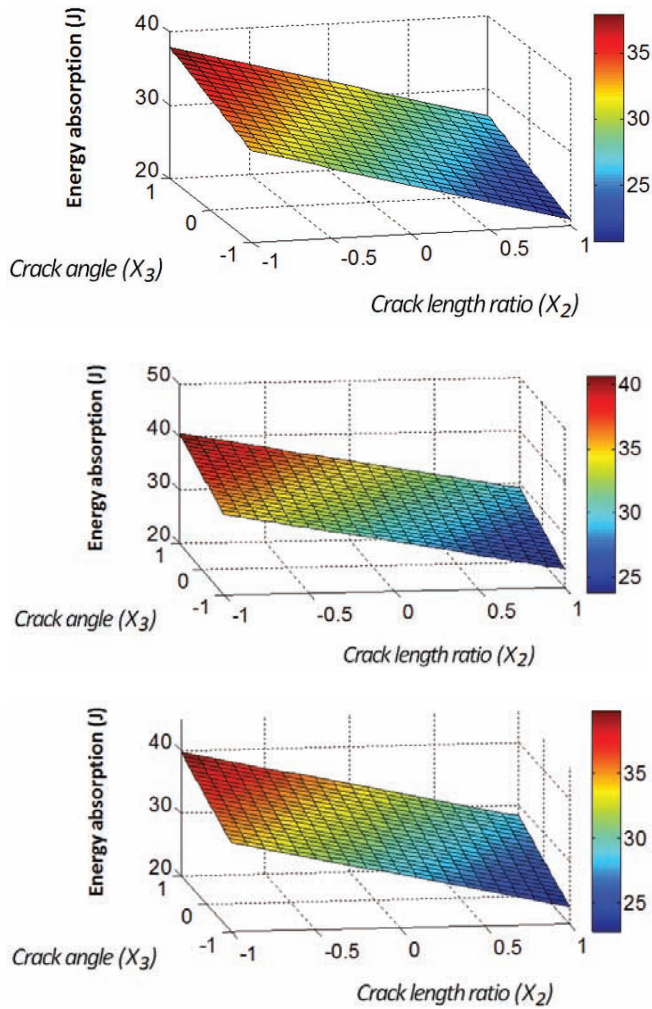


Figure 10. The effect of: (a) crack length ratio (X_2) and crack angle (X_3) on energy absorption value of the C1 type patches (the G-G-A lay-up); (b) crack length ratio (X_2) and crack angle (X_3) on energy absorption value of the C2 type patches (the A-G-G lay-up) and (c) crack length ratio (X_2) and crack angle (X_3) on energy absorption value of the C3 type patches (the G-A-G lay-up).

length ratio results in a reduction in the absorbed energy in the structure. This shows the negative role of the crack length on the energy absorption in the structure. One also sees that the effect of crack angle is linear. The more the crack angle is, the more energy absorbs in the structure.

Finally in Fig. 12, the effect of crack length ratio and FML patch type are shown for specimens having different crack angles (0° , 30° , or 45°). Figure 12 shows that the 3D obtained surface is nearly the same for different crack angles. The more the crack angle is, the more the height of the surface (amount of the absorbed energy in the structure) is. One also sees that the degree of the surface is 2, respect to the X_1 axis. The most positive effect of the C2 type patching could be seen here too.

6. CONCLUSIONS

By using design of experiments and applying response surface method, the impact behavior of repaired and un-repaired

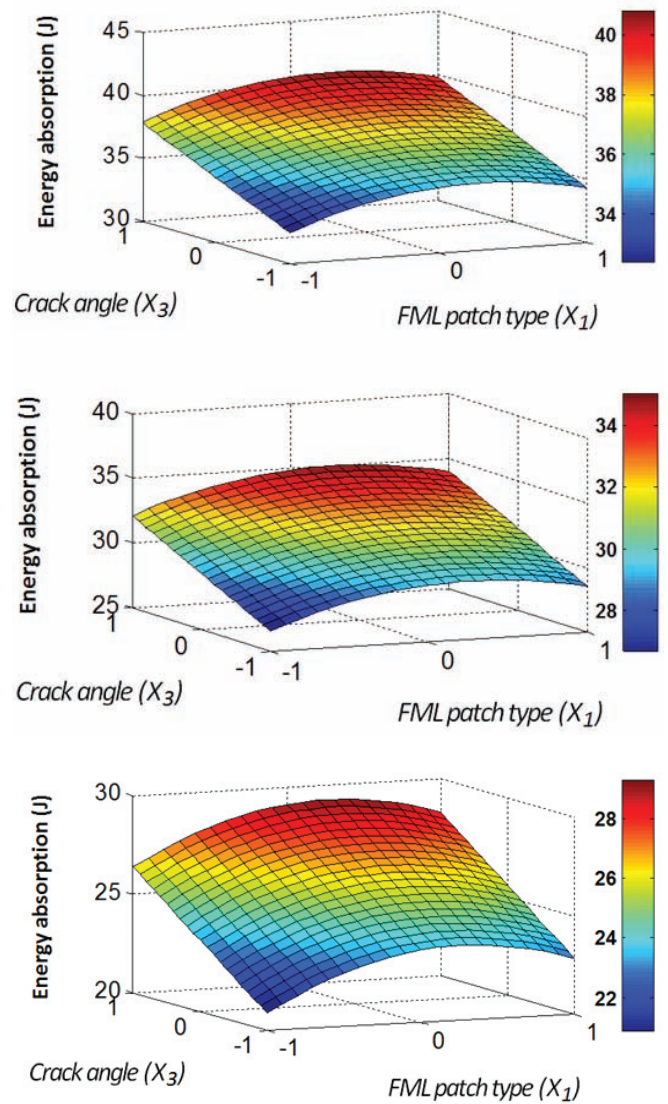


Figure 11. The effect of: (a) FML patch type (X_1) and crack angle (X_3) on energy absorption value for a crack length ratio of $a/w=0.1$, (b) FML patch type (X_1) and crack angle (X_3) on energy absorption value for a crack length ratio of $a/w=0.3$ and (c) FML patch type (X_1) and crack angle (X_3) on energy absorption value for a crack length ratio of $a/w=0.5$.

cracked aluminum plates was studied under Charpy tests. The desired parameters were composite patch lay-up, crack length, and crack angle each one in three levels. The significance and accuracy of the derived quadratic equation was evaluated. The results of the current work indicate that:

- (a) RSM is a reliable and powerful tool for modeling and optimization of the energy absorption of cracked or un-cracked plates. The presented 3D response surface graphs described a better understanding of the effects of the variables on the energy absorption.
- (b) Inconstant crack length ratios, when the crack angle increases, the absorbed energy in the structure increases too. Regardless of repairing the samples, if the crack length ratio increases, the strength of them reduces.
- (c) The major factors in the fracture surface of the unpatched

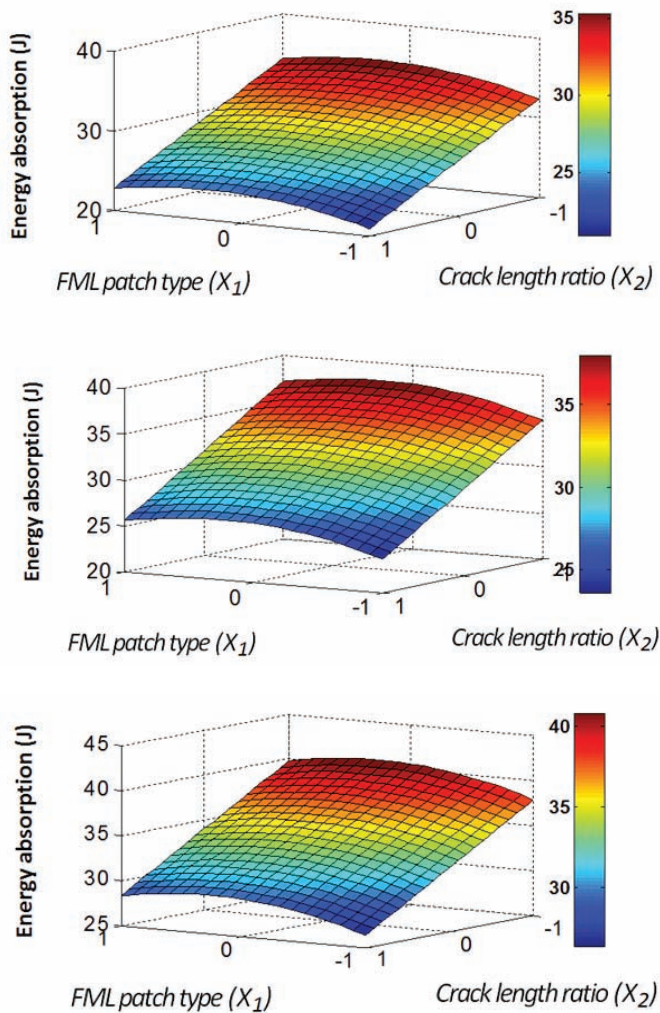


Figure 12. The effect of: (a) FML patch type (X_1) and crack angle (X_2) on energy absorption value for crack angle of $\theta=0^\circ$, (b) FML patch type (X_1) and crack angle (X_2) on energy absorption value for crack angle of $\theta=30^\circ$ and (c) FML patch type (X_1) and crack angle (X_2) on energy absorption value for crack angle of $\theta=45^\circ$.

cracked specimens were the cup and cone shear surfaces and plastic deformation. The main failure mechanisms in the patches are fiber breakage, fiber pull-out, and plastic deformation of the metal layer, respectively.

- (d) Regardless of the crack length ratio or the crack angle, the type of patch lay-up influences the strength of the repaired structures. Whatever the patch metal layer is close the repair surface, the absorbed energy increases in the structure.

REFERENCES

1. Khalili, S.M.R.; Ghajar, R.; Sadeghinia, M.; Mittal, R.K. & Mason, P. Effect of patching on Charpy impact response of repaired notched plate – experimental study. *J. Adhesion*, 2010, **86**, 561-85. doi: 10.1080/00218464.2010.484310
2. Schubbe, J.J. & Mall, S. Investigation of a cracked thick aluminum panel repaired with a bonded composite patch. *Eng. Fracture Mech.*, 1999, **63**, 305-323. doi: 10.1016/S0013-7944(99)00032-6
3. Wang X. Shape memory alloy volume fraction of pre-stretched shape memory alloy wire-reinforced composites for structural damage repair. *Smart Materials Structures* 2002;11: 590–595. doi: 10.1088/0964-1726/11/4/315
4. Belhouari, M.; Bachir Bouiadjra, B.; Megueni, A. & Kaddouri, K. Comparison of double and single bonded repairs to symmetric composite structures: a numerical analysis. *Composite Structures*, 2004, **65**, 47–53. doi: 10.1016/j.compstruct.2003.10.005
5. Tsai, G.C. & Shen, S.B. Fatigue analysis of cracked thick aluminum plate bonded with composite patches. *Composite Structures*, 2004, **64**, 79–90. doi: 10.1016/S0263-8223(03)00216-2
6. Ghosh, D.P.; & Gopalakrishnan, S. Coupled analysis of composite laminate with embedded magnetostrictive patches. *Smart Mater. Struct.*, 2005, **14**, 1462-73. doi: 10.1088/0964-1726/14/6/038
7. Toudeshki, H.H.; Mohammadi, B. & Daghyani, H.R. Mixed-mode fracture analysis of aluminium repaired panels using composite patches. *Composites Sci. Technol.*, 2006, **66**, 188–198. doi: 10.1016/j.compscitech.2005.04.028
8. Papanikos, P.; Tserpes, K.I. & Pantelakis, S.P. Initiation and progression of composite patch debonding in adhesively repaired cracked metallic sheets. *Composite Structures*, 2007, **81**, 303–311. doi: 10.1016/j.compstruct.2006.08.022
9. Ayatollahi, M.R. & Hashemi, R. Mixed mode fracture in an inclined center crack repaired by composite patching. *Composite Structures*, 2007, **81**, 264–273. doi: 10.1016/j.compstruct.2006.08.013
10. Khalili, S.M.R.; Ghadjar, R.; Sadeghinia, M. & Mittal, R.K. An experimental study on the Charpy impact response of cracked aluminum plates repaired with GFRP or CFRP composite patches. *Composite Structures*, 2009, **89**, 270–274. doi: 10.1016/j.compstruct.2008.07.032
11. Khalili, S.M.R.; Ghajar, R.; Sadeghinia, M.; Mittal, R.K. & Mason, P. Effect of patching on charpy impact response of repaired notched plate – experimental study. *J. Adhesion*, 2010, **86**, 561–585. doi: 10.1080/00218464.2010.484310
12. Pandey, P.C. & Kumar, S. Adhesively-bonded patch repair with composites. *Def. Sci. J.*, 2010, **60**(3), 320-329. doi: 10.14429/dsj.60.360
13. Box, G.E.P. & Draper, N.R. Response surfaces, mixtures and ridge analyses. Chapter 3, page 29, 2007, John Wiley & Sons, Inc., ISBN 978-0-470-05357-7. doi: 10.1002/9780470072769.ch3
14. ASM Handbook, Volume 2, Properties and Selection: Nonferrous Alloys and Special-Purpose Materials, ASM International, Metals Park, OH, 1990.
15. American Society for Testing and Materials (ASTM). ASTM E 8M-09, Standard test methods for tension testing of metallic materials, 2010.
16. ASTM D 2651, -American Society for Testing and Materials (ASTM), West Conshohocken, PA, USA, 1995 Standard guide for preparation of metal surfaces for adhesive bonding-2001.
17. Huntsman Advanced materials data sheet for Araldite LY5052-1 /Aradure 5052-1, www.huntsman.com/

- advanced_ materials, 2007.
18. Wegman RF. Surface preparation techniques for adhesive bonding. William Andrew Inc. NOYES publication; 1989.
 19. Huntsman Advanced materials data sheet for Araldite 2015, www.huntsman.com/advanced_ materials, April 2007.
 20. Clearfield, H.M.; McNamara, D.K. & Davis, G.D. Adhesives and sealants. *In* Engineered materials handbook, Edited by Brinson HF, Brinson H.F. Vol. 3. ASM International; 1990: 260.
 21. Toudeshki, H.H.; Mohammadi, B. & Bakhshandeh, S. Crack trajectory analysis of single-side repaired thin panels in mixed-mode conditions using glass/epoxy patches. *Computers Structures*, 2008, **86**, 997–1005. doi: 10.1016/j.compstruc.2007.04.015
 22. American society for testing and materials (ASTM). ASTM E23–02a, Standard test methods for notched bar impact testing of metallic materials-2002.

CONTRIBUTORS

Dr Faramarz Ashenai Ghasemi obtained his PhD (Mechanical Engineering-Design of Solids) from KNTU, Tehran, Iran. Presently he is working as an associate professor at Shahid Rajaei Teacher Training University (SRTTU), Tehran, Iran. His research interests include: Composite materials, impact mechanics, nano-composites, and mechanical behaviour of materials. In current study, he has guided in experimental study as his MS supervisor.

Mr Lotfali Mozaffari Vanani obtained his MS (Mechanical Engineering-Applied Design) from Shahid Rajaei Teacher Training University (SRTTU), Tehran, Iran. Presently he is working as a teacher in technical high schools in Iran. His research interests include: composite materials, fracture mechanics, and repairing of composite materials. This study is some part of his MS project.

Dr Ali Pourkamali Anaraki obtained his PhD (Mechanical Engineering-Applied Design) from Tarbiat Modares University, Tehran, Iran. Presently he is working as an associate professor at Shahid Rajaei Teacher Training University (SRTTU), Tehran, Iran. His research interests include: fracture mechanics, porous materials, fatigue, and simulation. In current study, he has guided in simulation study as his MS supervisor.

Dr Sadigh Raissi obtained his PhD (Industrial Engineering) from Islamic Azad University (IAU), Tehran, Iran. Presently he is working as an associate professor at School of Industrial Engineering in Islamic Azad University, Tehran South Branch (IAU-STB), Tehran, Iran. His research interests include: reliability engineering, statistical quality control, statistical process control, and computer simulation. In current study, he has guided in statistical modelling and optimisation study as his MS co-supervisor.